Applied Physics Letters

# Resistive spectroscopy coupled with non-contacting oscillator for detecting discontinuous-continuous transition of metallic films

Cite as: Appl. Phys. Lett. **111**, 101902 (2017); https://doi.org/10.1063/1.4995469
Submitted: 11 July 2017 . Accepted: 28 August 2017 . Published Online: 08 September 2017

**N. Nakamura, and H. Ogi**

# Resistive spectroscopy coupled with non-contacting oscillator for detecting discontinuous-continuous transition of metallic films

N. Nakamura[a] and H. Ogi
*Graduate School of Engineering Science, Osaka University, 1-3 Machikaneyama, Toyonaka Osaka 560-8531, Japan*

(Received 11 July 2017; accepted 28 August 2017; published online 8 September 2017)

In spectroscopic measurements, one measures responses of specimens to oscillating fields (including electric, magnetic, and stress fields) at different frequencies for characterizing the samples. In contrast, we develop spectroscopy where the response (loss) is measured by changing the electric resistance, named the resistive spectroscopy. In the resistive spectroscopy, an energy-loss peak appears when the resistance is changed. We here apply it for studying the morphological change of thin films. When a metallic material is deposited on a substrate, the morphological transition from discontinuous islands to the continuous film occurs. It accompanies a drastic change in the resistance of the deposited material because of the transition from an insulator to a conductor. We find that the energy-loss peak appears at the transition moment during deposition of Ag. The resistive spectroscopy we develop uses no electrodes; it adopts the electric field generated by a piezoelectric material vibrating at its resonant frequency beneath the substrate. It is observed that the full width at half maximum (FWHM) of the resonance shows the peak during the deposition for high resistance substrates. The FWHM peak fails to be found for low resistance substrates, but it appears when the resonance frequency is increased. We propose an electrical-circuit model for explaining these observations. *Published by AIP Publishing.* [http://dx.doi.org/10.1063/1.4995469]

Spectroscopy is generally used for materials characterization by measuring their responses to applied stimuli at different frequencies. Stiffness measurements using mechanical vibrations[1–3] and dielectric relaxation measurements[4,5] are examples of its applications. In contrast to the conventional spectroscopy, we here propose a spectroscopy method, where we change the electric resistance of the specimen instead of frequency and measure the energy loss as the response. To understand the mechanism of this unusual spectroscopy, it is helpful to consider two electrical circuits in Figs. 1(a) and 1(b). One is a series RLC circuit, whose impedance is $Z = R + i\omega L + 1/i\omega C$, where $R$, $L$, and $C$ are the resistance, inductance, and capacitance, respectively. The current $I$ and the energy loss $P$ in the circuit become maxima, when the angular frequency $\omega$ of the input ac voltage equals $1/\sqrt{LC}$. This is the resonant frequency, which can be normally found by sweeping frequency and measuring the responses. In contrast, when the resistance is changed at a fixed frequency, one peak appears in the $P$–$R$ relationship as shown in Fig. 1(c). Similar behavior is observed in the circuit as shown in Fig. 1(b), in which a resistor $R_1$ is connected to a parallel RLC circuit in series. When $R_1$ is changed, a maximum appears [Fig. 1(d)], and when $R$ is changed, a minimum appears [Fig. 1(e)]. Thus, the maximum or minimum usually appears in the $P$–$R$ relationship. We call materials characterization using this $P$–$R$ relationship the resistive spectroscopy. It must be noted that the resistive spectroscopy requires an extremely wide-range resistance change, like the change from an insulator to a conductor. However, such a wide and rapid resistance change does not happen normally.

We note that the drastic resistance change occurs during film growth. Nucleation, island growth, coalescence of islands, and formation of the continuous film are typical film-growth processes on substrates. When a metallic material is deposited, the insulator-to-conductor transition occurs in a short moment, which accompanies the drastic resistivity change.[6,7] We consider that the resistive spectroscopy is

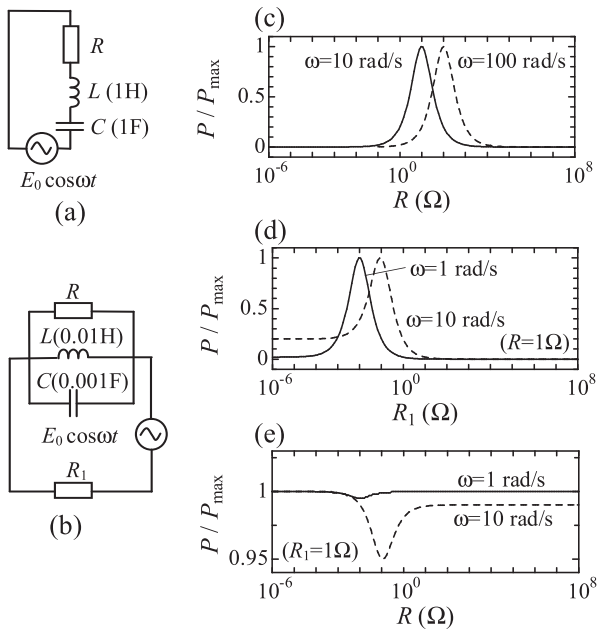


FIG. 1. Diagrams of (a) a series RLC circuit and (b) a circuit connecting a parallel RLC circuit and $R_1$ in series. $P$-$R$ relationships of circuit (a) are shown in (c) and those of circuit (b) are shown in (d) and (e). In (d), $R$ is fixed to be 1 Ω, and in (e), $R_1$ is fixed to be 1 Ω. $P$ is normalized by the maximum value $P_{max}$.

[a]Electronic mail: nobutomo@me.es.osaka-u.ac.jp

applicable to the detection of the transition. Recently, nanostructures that are obtained by stopping deposition around the transition are studied for fabricating hydrogen sensors,[8,9] transparent electrodes,[10] and films possessing temperature-independent resistivity,[11] because the nanostructures show unusual electrical properties. To obtain such nanostructures, a method that can detect the transition during deposition is required. The resistance measurement,[6] surface acoustic wave (SAW),[12–14] resonant ultrasound spectroscopy (RUS),[15] and a combination of surface differential reflectance spectroscopy and multiple-beam optical stress sensor[16] have been used for monitoring the film growth. The former three methods detect the resistance change caused by the morphological transition. In the resistance measurement and SAW method, electrodes are required on substrates, and in SAW and RUS, piezoelectric substrates are required. The last method requires no electrodes, but it cannot detect the transition clearly. In this letter, we develop a method based on the resistive spectroscopy. It detects the resistance change, but neither electrodes nor piezoelectric substrates are required. By using the method, the discontinuous-continuous transition of thin films is studied.

Figure 2(a) shows the schematic image of the experimental setup, which is simplified for explaining the measurement principle. A piezoelectric material is placed below a substrate, and a metallic material is deposited onto the top surface of the substrate. When the piezoelectric material oscillates mechanically, an electric field is generated around it. If the deposited material is located in the electric field, current flow and energy loss occur in the deposited film depending on its resistance. We propose an equivalent circuit for this system in Fig. 2(b). The piezoelectric material consists of a series RLC circuit ($R_P$, $L_P$, and $C_P$) and a capacitor $C'_P$. The substrate consists of a resistor $R_S$ and capacitor $C_S$, and the metallic film is a resistor $R_F$. The piezoelectric material and the film/substrate are connected in series. In this circuit, energy loss in the piezoelectric material changes depending on the resistance of the film. In other words, the change in the film resistance is detectable by monitoring attenuation of mechanical oscillations of the piezoelectric material.

We here calculate the energy loss in the equivalent circuit. In the following experiments, resonant spectra are measured by detecting the electric field generated around the oscillating piezoelectric material using the antennas, and a resonant frequency and full width at half maximum (FWHM) are determined from the spectra. To reproduce the measurement, we assume that the electric field measured by the antenna is proportional to that applied to the film/substrate $E_{F/S}$, and the relationship between $\omega$ and $|E_{F/S}|$ is calculated. Figure 3(a) shows reproduced spectra at different $R_F$. In the calculation, parameters are selected so as to cause resonance around $\omega_0 = 10^6$ rad/s.[17] As $R_F$ decreases, the resonant frequency $\omega_r$ decreases, and the FWHM becomes larger around $R_F = 10^7$ Ω. The detailed changes in $\omega_r$ and FWHM are plotted in Figs. 3(b) and 3(c), respectively. $\omega_r$ drop and FWHM peak are clearly observed around $R_F = 10^7$ Ω.

In the above calculation, relatively large resistance, $10^{12}$ Ω, is used for the substrate. For comparison, $\omega_r$ and FWHM are calculated for a substrate with lower resistance, $10^7$ Ω. The results are plotted in Figs. 3(b) and 3(c). Regarding $\omega_r$, it decreases as $R_F$ decreases. The behavior is similar to that observed for the high resistance substrate. In contrast, FWHM changes monotonically with $R_F$, and no peak appears, which indicates that the transition on the low-resistance substrate cannot be detected clearly. This behavior is understood intuitively as follows: As the resistance of the substrate becomes smaller, the current flow preferably occurs in the substrate rather than in the film, and the energy loss in the substrate is dominant in the total loss. After the continuous film is formed and the resistance of the film becomes lower than that of the substrate, the current flow is principally caused in the film, and the total energy loss becomes smaller. For these reasons, the peak does not appear. If the smaller resistance of substrate is the cause of the disappearance of FWHM peak, the peak should appear by increasing $\omega$; the increase in $\omega$ increases the impedance of the substrate. Calculation results at $5.0 \times 10^6$ rad/s for the low resistance substrate are plotted in Figs. 3(b) and 3(c), where $C_P = 4.0 \times 10^{-19}$ F is used to

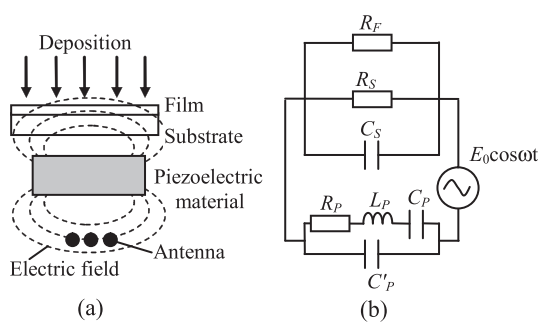


FIG. 2. (a) Schematic cross sectional view of the measurement setup and (b) the proposed equivalent circuit.

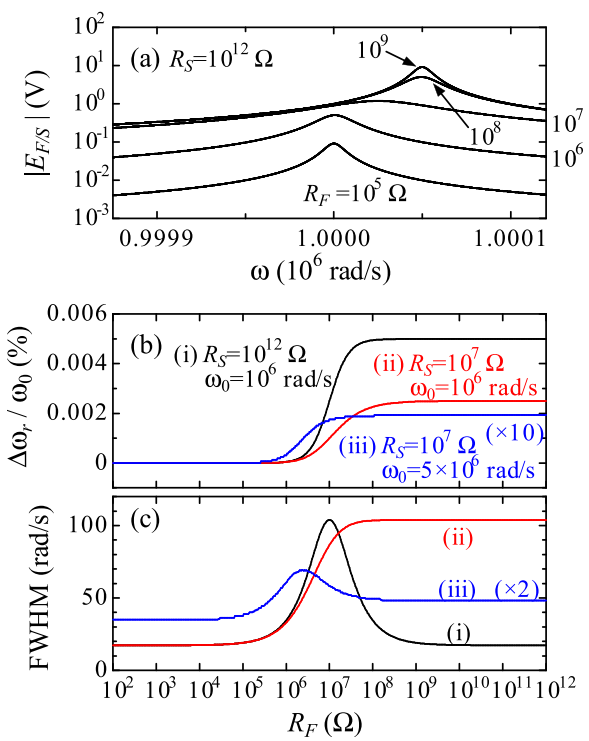


FIG. 3. Calculation results for the equivalent circuit. (a) Relationships between $|E_{F/S}|$ and $\omega$ at different $R_F$. (b) Change ratio of $\omega_r$ and (c) FWHM at different $R_S$ and $\omega_0$. Data at $R_S = 10^7$ Ω and $\omega_0 = 5 \times 10^6$ rad/s are enlarged.

increase the resonant frequency. Both the frequency drop and the FWHM peak appear as expected, and the transition should be detectable. Thus, we expect that the resistive spectroscopy can detect the morphological transition of the deposited material by controlling the frequency of the piezoelectric material.

In the following, we experimentally confirm this. Figure 4 shows the schematic of the measurement setup we developed, including the sensor and the substrate. Three line antennas are embedded in the nylon base, and the lithium niobate rectangular parallelepiped is placed on it. The substrate is placed on the Al holder so that the substrate does not contact with the lithium niobate. The measurement setup is placed in the RF-sputtering chamber, and Ag is deposited from above it. Resonant spectra are measured by using the antenna transmission acoustic resonance,[18,19] in which burst signals are applied to one of the antennas to oscillate the lithium niobate and the electric field excited by the oscillating lithium niobate is detected by one of the remaining antennas. By sweeping the driving frequency, the resonant frequency $f_r$ and FWHM are measured. The lithium niobate is a single crystal, measuring $2.5 \times 1.7 \times 0.2\,\mathrm{mm}^3$. The background pressure is less than $3.5 \times 10^{-4}$ Pa, and the pressure during deposition under Ar flow is 0.4 Pa. The gap between the substrate and the lithium niobate is about 30 $\mu$m. For comparison with the conventional resistance-measurement method, the Ag electrodes are formed on the substrate, and the resistance is measured during deposition. Four substrates, Si ($>10^4$ Ω cm), Si (~20 Ω cm), silica, and Al, are used in the following measurements. The thickness of the Al is 1 mm, and those of other substrates are 100 $\mu$m. Their in-plane dimensions are larger than those of the lithium niobate.

First, the effects of the substrate resistance on $f_r$ and FWHM are evaluated before deposition. Figure 5(a) shows representative resonant spectra, when different substrates are placed on the sensor. Changes of $f_r$ and FWHM depend on the substrate resistance; the largest and smallest decreases of $f_r$ are observed with Al and silica substrates, respectively. Figure 5(b) shows the changes in $f_r$ and FWHM when different resonant modes are measured. The frequency change, $\Delta f_r$, is normalized so that it becomes zero and unity when the frequencies are measured with and without the Al substrate, respectively. The normalized value represents the degree of the piezoelectric stiffening; a larger value indicates that the lithium niobate shows the stronger piezoelectric effect. ΔFWHM is the increase in FWHM by placing the substrate on the sensor, and it is also normalized by multiplying $1/(f_{\mathrm{LN}} - f_{\mathrm{Al}})$, which corresponds to internal friction $Q^{-1}$ normalized by the degree of the piezoelectric stiffening. Here, $f_{\mathrm{LN}}$ and

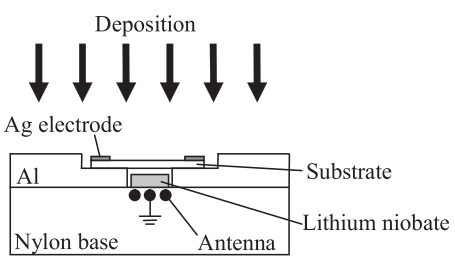


FIG. 4. Schematic of the measurement setup, including the sensor and substrate.

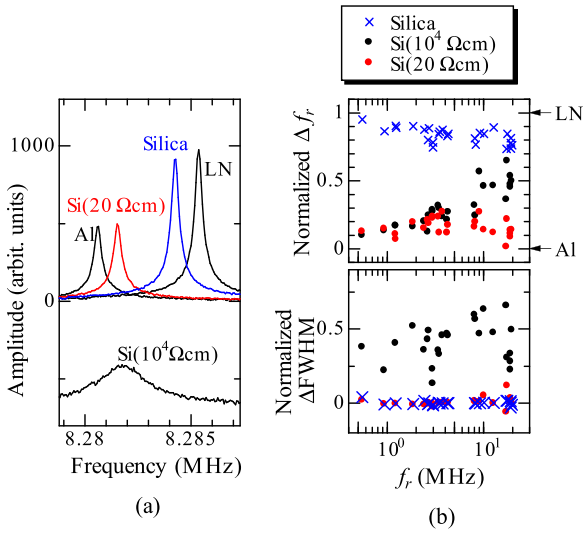


FIG. 5. Effect of the substrate on the resonant vibration of the lithium niobate. (a) Resonant spectra when different substrates are placed on the sensor. The spectrum for Si ($10^4$ Ω cm) is enlarged and moved in the vertical direction. (b) Changes in the resonant frequency and FWHM measured at different resonant frequencies.

$f_{\mathrm{Al}}$ are resonant frequencies measured without and with the Al substrate, respectively. Regarding the silica substrate, $\Delta f_r$ is nearly unity. When the low-resistance Si substrate (~20 Ω cm) is placed on the sensor, $\Delta f_r$ is less than 0.3, and notable frequency dependence is not observed, meaning that the substrate is regarded as a conductor. Regarding the high-resistance Si substrate ($>10^4$ Ω cm), $\Delta f_r$ increases as the resonant frequency increases. This result indicates that this substrate behaves like a conductor at lower frequencies and it transforms to an insulator as the frequency increases. Regarding the ΔFWHM, it is almost zero for the silica and the low-resistance Si substrate but shows larger values for the high-resistance Si substrate.

Film growth monitoring is then conducted. Figure 6(a) shows representative resonant spectra observed at different times during deposition on the silica substrate (detailed spectrum change is shown in the supplemental material). Figures 6(b) and 6(c) show the corresponding changes in $f_r$ and FWHM, respectively. $f_0$ is the resonant frequency just after opening the shutter. The inverse of resistance $R_E$ measured using the electrodes is also plotted. The resonance around 1.8 MHz is monitored. Deposition starts at 0 s by opening the shutter. In the early stage of deposition, notable changes are not observed in $f_r$ and FWHM. Around 1250 s, corresponding to the thickness of 9.5 nm, $f_r$ drops and FWHM shows a maximum. These behaviors agree with the calculation results for $R_S = 10^{12}$ Ω at $\omega_0 = 10^6$ rad/s in Fig. 3.

To understand the relationship between the FWHM peak and the transition, morphological change is evaluated by taking atomic-force microscopy (AFM) images and measuring surface roughness $R_a$. Four samples are prepared by stopping deposition at different times: two before the FWHM peak and the others after the peak. In the AFM images, before the FWHM peak, the in-plane island size increases with time [Figs. 7(a) and 7(b)], but after the FWHM peak, the island growth is not observed clearly [Figs. 7(c) and 7(d)]. Regarding $R_a$, it increases before the FWHM peak, but it

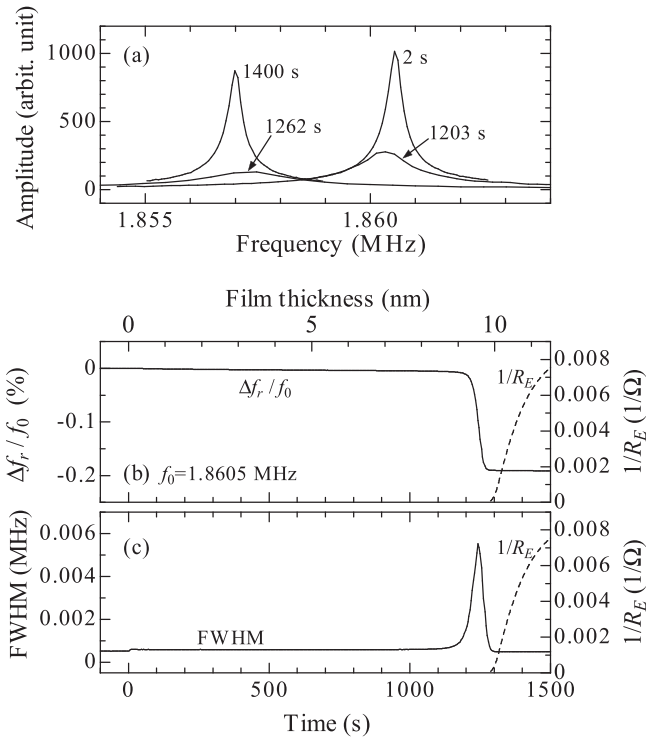


FIG. 6. Experimental results obtained by depositing Ag on the silica substrate. (a) Representative resonant spectra measured at different times, and changes in (b) resonant frequency and (c) FWHM during deposition. Inverse of the electric resistance is also plotted.

decreases gradually after the FWHM peak [Fig. 7(e)]. These results indicate that the in-plane island growth process almost completes at the FWHM peak, and deposited atoms migrate to grooves between islands, making the film surface flat, after the peak. Regarding $R_E$, it is not measurable in the early stage of deposition because of high resistivity. However, around the FHWM peak, it becomes measurable, and the conductivity, $1/R_E$, suddenly increases [Figs. 6(b) and 6(c)]. These results confirm that the transition occurs at the FWHM peak. Thus, the resistive spectroscopy detects the transition.

Figure 8 shows the experimental results for the high-resistance Si and the low-resistance Si substrates. When film

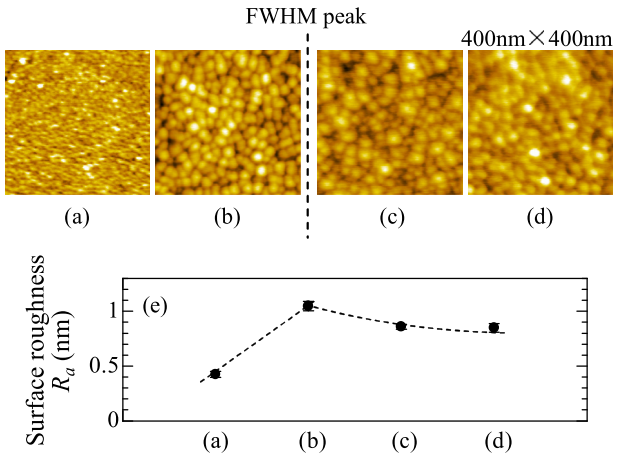


FIG. 7. AFM images of Ag films. The images are taken after stopping deposition (a) at 300 s, (b) after FWHM starts to increase, (c) during FWHM decreases after the FWHM peak, and (d) just after the FWHM peak appears. (e) Surface roughness measured from the AFM images. The dashed line is a guide to the eye.

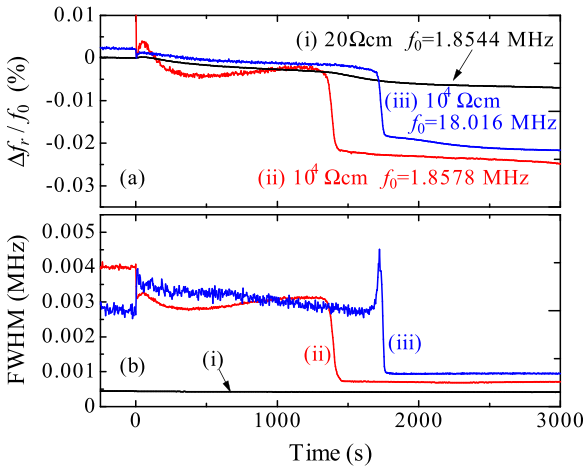


FIG. 8. Changes in (a) resonant frequency and (b) FWHM during deposition of Ag on Si substrates.

growth on the low-resistance Si substrate is monitored using the resonance around 1.8 MHz, $f_r$ decreases gradually with time, and the FWHM peak does not appear. The transition cannot be detected from these results. Regarding the high-resistance Si substrate, both $f_r$ and FWHM drop simultaneously at around 1400 s. These behaviors are similar to those observed for the low resistance substrate ($R_S = 10^7$ Ω, $\omega_0 = 10^6$ rad/s) in Fig. 3. According to the above calculation, by using higher frequencies, the FWHM peak should appear. To confirm the expectation, the experimental results, in which the resonance around 18 MHz is used for the high-resistance Si substrate, are shown in Fig. 8. The $f_r$ drop and the FWHM peak appear, showing good agreement with the calculation results ($R_S = 10^7$ Ω, $\omega_0 = 5 \times 10^6$ rad/s in Fig. 3). Thus, the resistive spectroscopy can identify the moment at which the transition occurs for the low resistance substrate by using higher resonant modes.

In the above experiments, film growth on the substrates with a thickness of 100 $\mu$m was monitored. Because the electric field generated around the oscillating piezoelectric material becomes weak with increasing the distance from the piezoelectric material, sensitivity to the morphological change should deteriorate with the increase in the substrate thickness. To confirm the available substrate thickness, we monitored film growth on glass substrates of different thicknesses up to ~1.1 mm. As the substrate thickness increased, the FWHM peak became smaller (see Fig. S1 in the supplementary material). The morphological transition on the ~1.1 mm substrate was detectable, but the FWHM peak was very small. Therefore, above the substrate thickness, detection will be difficult.

The resistive spectroscopy is applicable to substrates with low electric resistance by using higher frequencies. Using a smaller piezoelectric material is a way to make frequencies higher. When a millimeter-sized oscillator is used, measurable resonant frequencies are of the order of $10^7$ Hz, and substrates whose resistivity is larger than $10^4$ Ω cm will be available, as shown in this study. If micrometer-sized piezoelectric oscillators are used, the measurable minimum resistance will be smaller.

In the experiments, we sweep the driving frequency for measuring the resonance frequency and the loss of the

piezoelectric material repeatedly during deposition. One may consider that this is the same sequence as the conventional spectroscopy. However, the materials characterization is performed from the relationship between the energy loss and resistance, and the principle of the resistive spectroscopy is different from that of the conventional spectroscopy.

In conclusion, we developed a method that detects the discontinuous-continuous transition of the thin film. The sensor is quite simple, and the transition is detectable by placing the sensor beneath the substrate without contacting neither the substrate nor the film. These features are useful for practical applications. In this study, we investigated the relationship between the energy loss and electric resistance. However, the resistive spectroscopy should be applicable to the characterization of mechanical properties as well because the mechanical system is analogous to the electrical circuit.

See supplementary material for details of the change in the resonance during deposition of Ag and the effect of the substrate thickness on the FWHM peak.

The authors wish to thank Y. Shiraiwa for assistance in the experiment. This work was supported by Japan Society for the Promotion of Science KAKENHI Grant No. 15H05503.

[1]I. Ohno, J. Phys. Earth **24**, 355 (1976).
[2]A. Migliori, J. L. Sarrao, W. M. Visscher, T. M. Bell, M. Lei, Z. Fisk, and R. G. Leisure, Physica B **183**, 1 (1993).
[3]N. Nakamura, H. Ogi, and M. Hirao, J. Appl. Phys. **111**, 013509 (2012).
[4]F. S. Howell, R. A. Bose, P. B. Macedo, and C. T. Moynihan, J. Phys. Chem. **78**, 639 (1974).
[5]F. Stickel, E. W. Fischer, and R. Richert, J. Chem. Phys. **104**, 2043 (1996).
[6]I. M. Rycroft and B. L. Evans, Thin Solid Films **290–291**, 283 (1996).
[7]M. Nishiura and A. Kinbara, Thin Solid Films **24**, 79 (1974).
[8]O. Dankert and A. Pundt, Appl. Phys. Lett. **81**, 1618 (2002).
[9]T. Kiefer, L. G. Villanueva, F. Fargier, F. Favier, and J. Brugger, Appl. Phys. Lett. **97**, 121911 (2010).
[10]D. S. Ghosh, L. Martinez, S. Giurgola, P. Vergani, and V. Pruneri, Opt. Lett. **34**, 325 (2009).
[11]C. Bansal, S. G. Praveen, J. T. T. Kumaran, and A. Chatterjee, Sci. Rep. **5**, 7685 (2009).
[12]P. Bierbaum, Appl. Phys. Lett. **21**, 595 (1972).
[13]R. Wiegert, H. Yoshida, K. J. Sun, M. Levy, H. Salvo, Jr. Mcavoy, and B. R. Mcavoy, J. Phys. Colloq. **46**, C10–737 (1985).
[14]M. Takahashi, H. Shoji, and M. Tsunoda, J. Magn. Magn. Mater. **134**, 403 (1994).
[15]N. Nakamura, N. Yoshimura, H. Ogi, and M. Hirao, J. Appl. Phys. **118**, 085302 (2015).
[16]G. Abadias, L. Simonot, J. J. Colin, A. Michel, S. Camelio, and D. Babonneau, Appl. Phys. Lett. **107**, 183105 (2015).
[17]Following parameters are used; $R_P = 10^6\ \Omega$, $L_P = 10^5$ H, $C_P = 10^{-17}$ F, $C'_P = 10^{-16}$ F, $R_S = 10^{12}\ \Omega$, $C_S = 10^{-13}$ F, and $E_0 = 1.0$ V.
[18]H. Ogi, K. Motohisa, T. Matsumoto, K. Hatanaka, and M. Hirao, Anal. Chem. **78**, 6903 (2006).
[19]N. Nakamura, M. Sakamoto, H. Ogi, and M. Hirao, Rev. Sci. Instrum. **83**, 073901 (2012).